

An Algorithm for Automated Segmentation for Bleeding Detection in Endoscopic Images

Eva Tuba
Faculty of Mathematics
University of Belgrade
Studentski trg 16, Belgrade
SERBIA
etuba@ieee.org

Milan Tuba
Graduate School of Computer Science
John Naisbitt University
Bulevar umetnosti 29, Belgrade
SERBIA
tuba@ieee.org

Raka Jovanovic
Qatar Environment and Energy Research Institute
Hamad Bin Khalifa University
PO Box 5825, Doha
QATAR
rjovanovic@hbku.edu.qa

Abstract—Wireless capsule endoscopy is an important advanced diagnostics method. It produces huge amount of images during travel through patient's digestive tract and that usually requires automated analysis. One of the most important abnormalities is bleeding and automated segmentation for bleeding detection is an active research topic. In this paper we propose an algorithm for automated segmentation for bleeding detection in capsule endoscopy images. The algorithm uses block based segmentation where average saturation from the HSI model and skewness and kurtosis of uniform local binary patterns histogram are used as features for the support vector machine classifier. Support vector machine parameters are tuned using grid search. The proposed method was tested using standard benchmark images and compared with other approaches from literature using Dice similarity coefficient and misclassification error as metrics, where it obtained better results using simpler features.

I. INTRODUCTION

Many different scientific areas made significant progress since the digital images were introduced. Digital image processing is far simpler than processing analog images which results in simpler image analysis. During last decades numerous methods for digital image processing were proposed and used in different scientific fields with different aims. Image processing algorithms are used in astronomy [1], biology [2], criminology [3], etc. Medicine represents one of the fields that enjoy many benefits of digital images and digital images processing. Before digital images, medical images were manually looked at and examined by doctors. Human eye is not a perfect organ so many anomalies in images were easily disregarded or misinterpreted. Nowadays all images, even if they were not originally digital, can be transferred into digital images. Using image processing algorithms different features in images can be emphasized and used for further analysis. Especially in medicine, hidden anomalies can be found and it can help early diagnostics which is very important [4], [5], [6].

Numerous sources are used for creating medical digital images. Some of the well known sources are magnetic resonance imaging (MRI), computerized tomography (CT), positron emission tomography (PET) scan, X-rays, ultrasound, etc. Human body is a complicated mechanism, thus all these sources were needed in order that soft tissues as well as

bones could be filmed and used for further examination. X-ray is for example used for filming the bones, MRI is suitable for filming soft tissues such as brain, while ultrasound is useful for kidney, heart examination, etc. Medical digital image processing represents an active research field. The main goal of the algorithms for processing medical images is to detect anomalies in images with very often poor quality due to different types of noise [7]. After the necessary steps of image enhancement, anomalies detection can be performed. In most cases this task requires some kind of image segmentation [8], [9]. Besides medicine, image segmentation is common task in other image processing algorithms. Large number of methods for this problem were proposed [10], [11]. Algorithms for image segmentation usually depend on choosing optimal threshold value [12], [13], [14].

For better view and diagnostics modern technologies are very helpful in producing digital images. One of the examples is wireless capsule endoscopy. Capsule endoscopy (CE) is the name of the procedure where small wireless camera is used to collect large number of images of the entire digestive tract. This procedure has been commercially used in the last 15 years. Principle is that wireless camera that is inside vitamin size capsule should be swallowed by the patient. The camera takes thousands of images during the travel through digestive tract. These images are sent to the recorder that patient wears on the belt. CE enables doctors to see the parts of digestive tract that cannot or are difficult to be accessed by more traditional endoscopic procedures. One of the main issues with this procedure is that it produces enormous amount of images, usually around 50,000. All these images need to be examined. Manual analysis by physician can last for many hours, even days and it is subject to human error. On the other hand, such large amount of data is a good opportunity for machine learning algorithms [15].

Since the beginning of CE use, many different methods for automated CE image analysis were proposed [16], [17]. Most of the methods are focused on specific abnormality detection rather than detection of abnormalities in general. Some of the usual abnormalities that can be detected are lesion, bleeding, tumors, etc. Each anomaly has specific characteristics so it is necessary to carefully chose features for each of them. In

literature, several major topics on the CE procedure can be found such as video segmentation [18], image enhancement [19] and disease detection [20], [21].

Bleeding represents one of the most common problems in digestive tract and further more, other diseases usually have bleeding as a consequence. In this paper we propose an automated bleeding detection in CE images using HSI color information and local binary patterns as features and support vector machine (SVM) as a classifier. CE images were divided into regions that were classified as blood, non-blood or background region by support vector machine. SVM was trained on manually selected and labeled regions. Pixel level precision is reached by voting method of overlapping blocks. Pixel was labeled with the label of the majority of blocks that it belongs to. Results of our proposed method were compared with algorithm proposed in [22].

The rest of the paper is organized as follows. In Section II a brief literature review is given. In Section III description of our proposed algorithm is given. It contains information about used features as well as information about SVM classifier. Section IV shows experimental results. Performance comparison of our proposed method with other approaches was done. At the end in Section V conclusion and suggestions for further work are given.

II. RELATED WORK

Capsule endoscopy image processing is widely researched topic. It represents a challenging problem because many different abnormalities can be searched for. In this paper we propose a method for bleeding detection, however besides that different tumors, lesions, polyps and other abnormalities can be detected by proper adjustment. All these different abnormalities have their own characteristics thus it would be very difficult to make a system that would recognize all abnormalities and classify them. The first step is to find methods that will recognize each of them, so later some combination can be used for detection and classification of all the abnormalities that can be seen in CE images.

In [23] an unsupervised method for the detection of polyps in CE videos was presented. Proposed method included watershed segmentation with initial marker selection method based on Gabor texture features and K-means clustering. Final extraction of polyp candidates from the resulting segments was done with curvature-based geometric information.

Similar method was proposed in [24] for detecting polyps and small bowel ulcers. The methodology was also based on log Gabor filters, but it was used for extracting the dominating texture leaving the background as non-significant texture. SUSAN edge detector was used for finding the boundaries after the geometric characteristic such as curvature and eccentricity were used for final polyp detection. As disadvantage of this method authors named the complexity which made it impossible to work in real time.

A method that used a combination of local features for detection of one of the most common intestinal diseases, ulceration, was proposed in [25]. Described method was based

on bag-of-words model with feature fusion technique. Image patches were determined by local binary pattern and SIFT features. The images were represented by the pyramid bag-of-words employed to model. Support vector machine classifiers were trained and at the end feature fusion technique was employed to determine a final conclusion. Reported experimental results showed that the described model outperforms single feature methods and other existing methods.

Alternative scheme for detection ulcer in capsule endoscopic images was presented in [26]. This approach used colortexture features to investigate how the structure information of healthy and abnormal tissue was distributed on RGB, HSV and CIE Lab color spaces. The CE images were initially pre-processed by bi-dimensional ensemble empirical mode decomposition. Based on experimental results, proposed scheme achieved classification mean accuracy over 95%.

Another abnormality that can be detected by CE is Crohn's disease. In [27] assessment of discrete disease for lesions created by mucosal inflammation in Crohn's disease (CD) was described. In that paper supervised classification, classifier cascade to classify discrete lesions and quantitative assessment of lesion severity was explored. Authors tested proposed method on database of 47 studies and the method showed high agreement with ground truth severity ratings manually assigned by an expert.

Paper [28] proposes a method for automatic recognition of tumor in CE images. Uniform local binary pattern as color texture feature with wavelet transform was proposed to characterize CE images. Features were chosen to be invariant to illumination change as well to describe multiresolution characteristics of the images. In order to refine the method, further feature selection was done. It was experimented with two feature selection approaches. The first one was based on support vector machine, sequential forward floating selection and the second one used recursive feature elimination. The proposed computer-aided diagnosis method achieves accuracy of 92.4% for tumor recognition in CE images.

In [29] method for automated hookworm disease detection in CE images was proposed. Gradient space named hybrid color gradient was developed. For gradient space analysis of the characteristics of hookworm infection images was done. Contourlet transformation was used for final features extraction. For classification the SVM was used.

An algorithm for bleeding detection in CE images was proposed in [30]. The proposed method was mainly based on color features since it is also an effective clue that physicians use for diagnostics. Described algorithm uses six color features in HSI color space. These color features were used to differentiate bleeding and normal status of organs. After feature extraction support vector machine was used as classifier to verify the performance of the chosen features. Status of the images were judged by the classifier. Authors reported that proposed method has average accuracy approximately 97%.

Another approach for bleeding detection was described in [31]. An algorithm that extracts color features from image-regions was proposed. Used color features were mean, stan-

standard deviation, skew and energy from the first order region histogram of the each RGB plane. The idea is to use three times the number of features that in the case of a gray scale image. In the mentioned paper the named features or better to say all possible combinations of features for classification were used and accuracy of the model was reported. The highest accuracy of the proposed algorithm was 89%.

In [32] another method for automatic bleeding detection in CE images was described. In proposed a method where a combination of color and spatial features were used. Series of descriptors that combine features were designed so the local and global features were incorporated together. Performance of the descriptors was verified by a kernel based classification method that used histogram intersection or chi-square.

Simpler model for bleeding detection based on image histograms was proposed in [33]. In that paper YIQ color plane was used, because it offers scope of utilizing human color-response characteristics. It was found that histogram patterns of bleeding and non-bleeding images in Y, I, and Q planes, have significant differences. Frequency values of three histograms were used in cascade to obtain desired feature vector. For classification, supervised K nearest neighbor classifier was used. Experimental results proved that proposed method provide very good results.

III. THE PROPOSED METHOD

Wireless capsule endoscopy camera creates color images. That fact enables the use of color features that can reveal more details in the image than gray scale images. Physicians also use color and texture features when examining images which is one more reason to try to use these features in computer-aided system for abnormality detection, especially bleeding.

In computer graphics different color spaces are used. For examination of color features the first task is to choose the adequate color space. One of the most popular color system is RGB model. When images are shown on the computer screen they are usually represented in RGB space because it is compatible with additive color reproduction systems. On the other hand, it was concluded that RGB space is often not most suitable for image processing. In this paper we use the HSI color space. In this color space hue and saturation describe chrominance, while luminance is represented as intensity. Each pixel is described by these three components (hue, saturation and intensity). Dominant color is defined by hue component, while saturation measures colorfulness. HSI color space is also suitable because it has been shown that it is color invariant, e.g. the same Euclidian distance correspond to the same perceiving differences of human eyes in any part of the color space.

In Fig. 1 examples of CE images with bleeding are shown. It can be seen that the color of blood is more vivid than the color of the tissue. That difference can be best seen in saturation component of the HSI model so we used it as the key component in our proposed approach. Second difference is in color intensity. We used intensity channel for extracting the texture features. In this paper we used uniform local binary patten (LBP) for describing the texture.

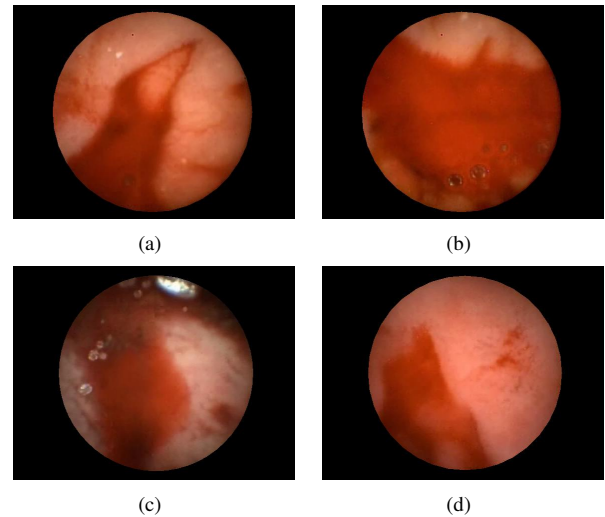


Fig. 1. Example of bleeding in CE images

LBP is a very simple, but powerful descriptor of the texture. The idea is to summarize local structure into a binary code. Central pixel is used as a threshold value for neighbor pixels. If the intensity value of the pixel is higher or equal than a central pixel, it is set to one, otherwise it is set to zero. Formal definition is given by the following expression:

$$s(i) = \begin{cases} 1, & \text{if } p(i) \geq p \\ 0, & \text{otherwise} \end{cases} \quad (1)$$

where p is the intensity value of the central pixel and $p(i)$ represents intensity of neighbor pixel i . New values of the neighbor pixels can be read in some order, usually clockwise direction in order to get binary pattern. Basic version of local binary pattern uses 3×3 neighborhood. In this case, binary pattern will be an 8 digit binary number so it will describe up to $2^8 = 256$ different local texture patterns. If the 5×5 neighborhood is chosen, the number of patterns is 2^{16} . In literature differently chosen neighborhoods can be found, but in our case the 3×3 neighborhood provided enough information.

Binary patterns can be transformed into decimal numbers. As mentioned before, for a 3 neighborhood 256 different patterns can be differentiated so the decimal number will be in the range $[0, 255]$. Based on patterns obtained from the image a histogram can be made. This histogram represents occurring frequency of each pattern. In this case histogram would be represented as a 256-dimensional vector. Dimension of the vector can be reduced by one of the most useful modifications of the basic LBP operator, uniform pattern. Uniform LBP pattern is rotation invariant feature. It groups all patterns that have more than two transitions from 0 to 1 or from 1 to 0 as one pattern. In this case instead of 256 patterns, only 59 will remain. There are 58 patterns with less than two transition and one is for all others.

In our proposed algorithm we calculated histogram for uniform LBP on regions 8×8 . That size was empirically

determined. Some characteristics of histogram are used as texture features. In this paper we tested the mean, variance, skewness, kurtosis, energy and entropy of the LBP histogram. Classification was done for all regions of that size in the image. Starting from the upper left corner mask region 8×8 was considered. For each region uniform local binary pattern and average saturation was determined. These characteristics were used as input features for the SVM. Support vector machine model was trained to label regions as region with or without bleeding or as background region. For input image all regions 8×8 are labeled. This procedure segments the image to region size level. Further analysis refines result to pixel level. For that, voting system was used. Except for the pixels at the edge, each pixel belongs to 64 different regions. Pixel will be label based on majority labels of the regions that it belongs to. In case of tie result, neighbor pixels are considered. For the edge pixels the same procedure is used, but their majority is not 33. Depending on the position at the edge it can belong to only one, two or more regions.

One of the latest and most successful classifiers is support vector machine (SVM). Basic SVM is a binary classifier, but it is widely used as multiclassifier. Using *one against one* or *one against all* methods any binary classifier can be used for multiclassification. *One against all* method builds models for each class that differentiate that class from all others, while in *one against one* procedure, one model for all pairs of classes is built. Final decision can be made in different ways. One simple method is by voting. Nowadays, support vector machines software has built-in system for multiclassification. We used LibSVM [34] for training SVM. In this software, one against one method is used.

The main idea for SVM is to find a hyperplane that separates instances from different classes assuming that that all instances must be on the right side of the hyperplane. This definition of SVM uses so-called hard margin.

However, real world problems almost always contain some number of outliers that are significantly different from other instances of the same class. For making SVM usable for real world problems instead of hard margin, soft margin was introduced. Formally, the following definition of hyperplane is used:

$$y_i(w \cdot x_i + b) \geq 1 - \epsilon_i, \quad \epsilon_i \geq 0, \quad 1 \leq i \leq n \quad (2)$$

where x_i refers to instances, $y_i \in \{-1, 1\}$ are corresponding labels of these instances, b is an intercept term, w denotes the normal vector to the hyperplane, d is the dimension of input vector, n is the number of input data (instances), while ϵ_i denotes slack variables. Slack variables allow instances to fall off the margin. For finding the optimal soft margin it is necessary to solve the following quadric programming problem:

$$\min \frac{1}{2} \|w\|^2 + C \sum_{i=1}^n \epsilon_i, \quad (3)$$

where C represents parameter of the soft margin cost function. Quality of the SVM model highly depends on the choice for this parameter. Larger values for C would make a model similar to the one made with a hard margin definition, while too small values for C would allow for too many instances to be misclassified.

Another problem that occurs is that basic SVM can work only with linearly separable data. Real world data very often do not have this characteristic. In order to overcome this problem kernel trick was introduced. Kernel trick replaces dot product with kernel function. Radial basis function (RBF) often used as kernel function is defined by the following equation:

$$K(x_i, x_j) = \exp(-\gamma \|x_i - x_j\|^2). \quad (4)$$

Parameter γ is free parameter that has significant impact on classification accuracy. This parameter defines influence of a single training example, e.g. for low values of γ influence reaches far while for the high values the reach is close. It can be said that γ is the inverse of radius of influence of samples that are chosen as support vectors.

In order to achieve the best accuracy, these parameters need to be tuned. In our proposed algorithm we used grid search which represents one of the simplest method for parameter tuning. Logarithmic search space was used as it was proposed in [35]. For models built during grid search only training set was used. For quality testing cross validation was done with 5 subsets. In order to further refine the proposed method, two-stage grid search was used. The first stage range for parameter C was $[-5, 15]$ with step 2, while for γ the used range was $[-15, 5]$, also with step 2. At the second stage, search range was reduced to neighborhood of the obtained best parameter values and step was reduced. Ranges are $Best_C \pm 3$ and $Best_\gamma \pm 2$ with step 0.5. Grid search with cross validation is a very simple method, but computationally expensive. This would be a problem if it should be done for each classification. However, adequate model need to be made just once. After the training of the SVM model, there is no need for this procedure thus the computation cost is not large.

Our proposed algorithm is summarized in Algorithm 1.

Algorithm 1: The proposed algorithm

Input : CE image

Step 1: Preparation: Transfer image form RGB model to HSI color model;

Step 2: Feature extraction: For regions 8×8 average saturation and uniform LBP histogram characteristics are calculated;

Step 3: Classification of regions: Each region is classified as blood, non-blood or background region by SVM;

Step 4: Pixel level classification: Each pixel is classified in one of three classes based on class of the regions that it belongs.

Output: Segmented CE image

IV. EXPERIMENTAL RESULTS

Experiments were performed on computer with the following characteristics: Intel® Core™ i7-3770K CPU at 4GHz, 8GB RAM, Windows 10 Professional OS. The proposed method was implemented in Matlab version R2016b and for support vector machine LIBSVM (Version 3.21) was used [34].

In this paper for testing of our proposed algorithm 50 CE images with bleeding were used. Dataset is free and online available [36]. Besides CE images, in this dataset ground truth images are given. Ground truth images were obtained with physician control. For training of the SVM 100 regions of each class (bleeding, non-bleeding and background) were used. Regions for training set were selected manually. After the SVM model was built, all the images were segmented using that model.

In order to measure the accuracy of the proposed method several evaluation metrics were used. These metrics were also used in [22]. The first metrics was Dice similarity coefficient [37]. This coefficient represents spatial overlap index which gives the measurement of similarity between two segmented images. In our case, image obtained by our proposed method was compared with ground truth. Dice similarity coefficient is defined by the following equation:

$$DSC = \frac{2 \cdot |F_g \cap F_t|}{|F_g| + |F_t|} \quad (5)$$

where F_g is pixel of ground truth and F_t is pixel of test image, $|x|$ represents cardinality of the set. If the DSC is equal to 1, segmentation is perfect.

Second evaluation metrics that was used is misclassification error. This metrics calculates the percentage of misclassified pixels. Definition of this metrics is given by the following equation:

$$MR = 1 - \frac{|B_g \cap B_t| + |F_g \cap F_t|}{|B_g| + |B_t|} \quad (6)$$

where B_t and F_t represent background and foreground pixels of the test images, while B_g and F_g are pixels of ground truth. The accuracy of segmentation is maximal in the case when MR is equal to 0.

In Table I average value and standard deviation for earlier mentioned features are shown. These characteristics were calculated from the instances of the training set. In the first column average value and standard deviation for instances that belong to class blood are presented, in the second column are characteristics for non-blood class and in the last column for background instances. Based on the results of this experiment some feature selection can be done. As it can be seen, average saturation of the regions is very different for instances between classes and also standard deviation for each class is small, which means that inside class instances are very similar. This qualifies this characteristics of regions for one of the features that will be used as input for the SVM. On the other hand, mean and variance of the LBP histogram are very similar for

blood and non-blood regions, while the background region is distinguished. For each tested characteristics background is clearly different than the actual tissue and because of that, each characteristics can be used to separate background from tissue. It could be assumed that the blood and non-blood regions could be differentiated by texture of blood and tissues, but this experiment shows that is not quite true. These two characteristics do not provide enough information.

TABLE I
COMPARISON OF USED FEATURES BETWEEN DIFFERENT CLASSES

| | | blood | non-blood | background |
|--------------|-----|----------|-----------|------------|
| Avg. satur. | avg | 0.7033 | 0.2806 | 1.0000 |
| | std | 0.1560 | 0.0825 | 0.0000 |
| LBP mean | avg | 0.0073 | 0.0075 | 0.0039 |
| | std | 0.0011 | 0.0011 | 0.0001 |
| LBP variance | avg | 0.2565 | 0.2587 | 0.2500 |
| | std | 0.0068 | 0.0072 | 0.0000 |
| LBP skewness | avg | 14.0695 | 13.5367 | 15.9046 |
| | std | 1.2236 | 1.2801 | 0.0108 |
| LBP kurtosis | avg | 211.1966 | 198.2581 | 253.9702 |
| | std | 30.8064 | 32.1944 | 0.2311 |
| LBP energy | avg | 0.3418 | 0.3344 | 0.9957 |
| | std | 0.0992 | 0.1063 | 0.0334 |
| LBP entropy | avg | 2.4883 | 2.3968 | 0.0167 |
| | std | 0.5055 | 0.5998 | 0.1291 |

Based on information in Table I we tried segmentation by SVM where only average saturation was used as feature of regions. Even though the difference between blood and non-blood region looks good enough it was not sufficient. In Fig. 2 segmentation with one feature (average saturation) as input for the SVM is shown. The segmentation was not done properly. For the shown example DSC is 0.7772 and MR is 0.1096 which are not good results. This proves that average saturation cannot be used as the only input feature, but it also shows that it is a good candidate. The main problem remains to find good features to describe blood and non-blood regions. In the case of the average skewness and kurtosis difference exists, but in both cases, standard deviation is relatively large. We can see that the values have overlapping intervals. These two characteristics could be used but with some additional features while average saturation has already been establish as a potentially good candidate.



Fig. 2. (a) Segmentation by SVM with only average saturation as input, (b) ground truth

In order to improve the quality of the SVM we used, besides tested average saturation, skewness and kurtosis. With these three features of regions, SVM was able to build satisfactory model.

Our proposed method was compared with method proposed in [22] where segmentation algorithm based on GrowCut for bleeding detection in CE images was proposed. Instead of the manual seed input, the proposed automated GrowCut (AGC) algorithm used clustering. Initially image was roughly segmented by dividing it into 5 to 15 clusters. After that the optimal number of clusters was obtained by Davies-Bouldin criterion. The cluster centroids subsequently labeled as bleeding, non-bleeding and background by a trained SVM classifier were used as seeds. Pixels that has RGB components around these centroids within some threshold were also used as seeds for the GrowCut segmentation, but not before the seed pruning step. In this step threshold value was used to discard incorrectly labeled seeds. Cluster that has less seeds than threshold value were not considered as seeds anymore.

Our proposed algorithm uses only 3 simple and easy to

compute features as input for the SVM classifier. Segmentation was later done by using SVM model that was previously built.

Our proposed method, even though it uses rather simple features, was able to outperform more complicated methods from literature. In Table II values for DSC (the best results are in bold) are shown.

TABLE II
COMPARISON OF DSC OBTAINED BY OUR PROPOSED METHOD (GRID-SVM) AND METHOD PROPOSED IN [22]

| | AGC | Grid-SVM1 | Grid-SVM2 |
|---------|-------------|-------------|--------------------|
| Min | 0.62 | 0.65 | 0.66 |
| Max | 0.97 | 0.97 | 0.98 |
| Average | 0.81 ± 0.09 | 0.82 ± 0.11 | 0.84 ± 0.10 |

In the first column are results reported in [22]. Last two columns represent results obtained by our proposed method

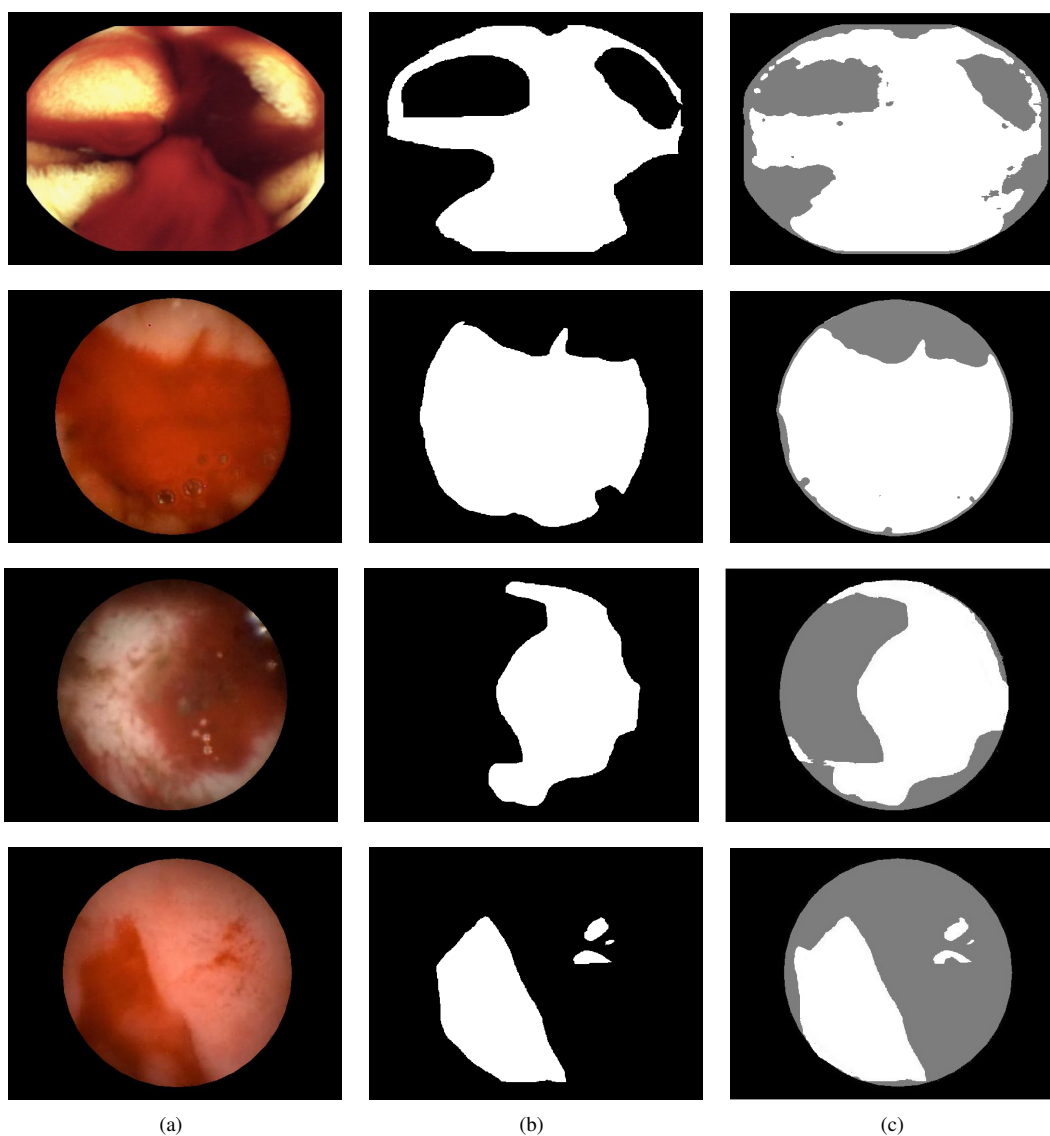


Fig. 3. Segmentation by our proposed algorithm: (a) CE images, (b) ground truth and (c) our proposed segmentation

at the first and second stage of the grid search. At the first stage of grid search the best parameter values were $C = 14$ and $\gamma = -12$. At the second stage, best fit was for $C = 13.5$ and $\gamma = -12$ with average accuracy of 98.44%. As it can be seen our proposed method achieved average DSC 0.84 while in [22] the best DSC was 0.81.

In Table III values for MR are given. Our proposed algorithm achieved average MR lower than the mentioned method from the literature (perfect segmentation is for $MR = 0$).

TABLE III
COMPARISON OF MR OBTAINED BY OUR PROPOSED METHOD (GRID-SVM) AND METHOD PROPOSED IN [22] (AGC)

| | AGC | Grid-SVM1 | Grid-SVM2 |
|---------|------------------|------------------|------------------------------------|
| Min | 0.009 | 0.009 | 0.007 |
| Max | 0.246 | 0.219 | 0.196 |
| Average | 0.095 ± 0.05 | 0.095 ± 0.05 | 0.093 ± 0.04 |

The proposed method in [22] was compared with other methods from literature [38] and reported significantly better results. Based on that and results in Table II and Table III, we can conclude that our proposed method for bleeding detection in CE images by support vector machine and color and texture features is very efficient since with rather simple features used it outperformed [22] and indirectly [38].

In Fig. 3 examples of segmentation by our proposed algorithm are shown. Ground truth images label just bleeding, while our proposed method differentiates bleedings, non-bleeding tissue and background. Black parts are background, gray non-bleeding tissue and white represents bleeding. Used metrics already showed that performance of our proposed method are good. In Fig. 3 visual quality can be seen. Segmentation with our proposed algorithm was very similar to ground truth. Some minor difference can be seen on the edges.

V. CONCLUSION

Capsule endoscopy represents one of the very useful methods in medicine. Huge amount of images that are produced by this procedure need some method for automated CE image analysis. In this paper, rather simple but very efficient method for automated blood detection in CE images was proposed. Proposed algorithm uses local binary pattern, color features and support vector machines as classifier. CE images were divided into regions 8×8 that were classified as blood, non-blood or background region by support vector machine. Average saturation and two characteristics of the uniform LBP histogram, skewness and kurtosis, were used for describing the regions. SVM had 3-dimensional input vector and 3 possible output classes. SVM was trained on manually selected and labeled regions based on ground truth. Pixel level precision was reached by voting method. Our proposed method that uses simple features outperformed existing more complicated methods in literature. As future research principal component analysis can be used for feature selection. Also some other texture features can be tested as well as detection of other abnormalities. SVM parameter tuning can be done more

efficiently using swarm intelligence algorithms rather than grid search.

ACKNOWLEDGMENT

This research is supported by the Ministry of Education, Science and Technological Development of Republic of Serbia, Grant no. III-44006.

REFERENCES

- [1] M. J. Aschwanden, "Image processing techniques and feature recognition in solar physics," *Solar Physics*, vol. 262, no. 2, pp. 235–275, 2010.
- [2] N. S. K. Gunda, H.-W. Choi, A. Berson, B. Kenney, K. Karan, J. G. Pharoah, and S. K. Mitra, "Focused ion beam-scanning electron microscopy on solid-oxide fuel-cell electrode: Image analysis and computing effective transport properties," *Journal of Power Sources*, vol. 196, no. 7, pp. 3592 – 3603, 2011.
- [3] V. Christlein, C. Riess, J. Jordan, C. Riess, and E. Angelopoulou, "An evaluation of popular copy-move forgery detection approaches," *IEEE Transactions on information forensics and security*, vol. 7, no. 6, pp. 1841–1854, 2012.
- [4] A. Stojak, E. Tuba, and M. Tuba, "Framework for abnormality detection in magnetic resonance brain images," in *24th Telecommunications Forum TELFOR*. IEEE, 2016, pp. 687–690.
- [5] H. Lee and Y.-P. P. Chen, "Image based computer aided diagnosis system for cancer detection," *Expert Systems with Applications*, vol. 42, no. 12, pp. 5356–5365, 2015.
- [6] M. Nikolic, E. Tuba, and M. Tuba, "Edge detection in medical ultrasound images using adjusted Canny edge detection algorithm," in *24th Telecommunications Forum TELFOR*. IEEE, 2016, pp. 691–694.
- [7] F. Latifoglu, "A novel approach to speckle noise filtering based on artificial bee colony algorithm: An ultrasound image application," *Computer methods and programs in biomedicine*, vol. 111, no. 3, pp. 561–569, 2013.
- [8] J. Mitra, P. Bourgeat, J. Fripp, S. Ghose, S. Rose, O. Salvado, A. Connelly, B. Campbell, S. Palmer, G. Sharma *et al.*, "Lesion segmentation from multimodal MRI using random forest following ischemic stroke," *NeuroImage*, vol. 98, pp. 324–335, 2014.
- [9] R. M. Stephen, A. K. Jha, D. J. Roe, T. P. Trouard, J.-P. Galons, M. A. Kupinski, G. Frey, H. Cui, S. Squire, M. D. Pagel *et al.*, "Diffusion MRI with semi-automated segmentation can serve as a restricted predictive biomarker of the therapeutic response of liver metastasis," *Magnetic resonance imaging*, vol. 33, no. 10, pp. 1267–1273, 2015.
- [10] M. Tuba and I. Brajevic, "Modified seeker optimization algorithm for image segmentation by multilevel thresholding," *International Journal of Mathematical Models and Methods in Applied Sciences*, vol. 7, no. 4, pp. 370–378, 2013.
- [11] S. Alpert, M. Galun, A. Brandt, and R. Basri, "Image segmentation by probabilistic bottom-up aggregation and cue integration," *IEEE Transactions on Pattern Analysis and Machine Intelligence*, vol. 34, no. 2, pp. 315–327, 2012.
- [12] M. Tuba, "Multilevel image thresholding by nature-inspired algorithms—A short review," *The Computer Science Journal of Moldova*, vol. 22, no. 3, pp. 318–338, 2014.
- [13] I. Brajevic and M. Tuba, "Cuckoo search and firefly algorithm applied to multilevel image thresholding," in *Cuckoo Search and Firefly Algorithm: Theory and Applications*, LNCS, X.-S. Yang, Ed. Springer International Publishing, 2014, pp. 115–139.
- [14] A. Alihodzic and M. Tuba, "Improved bat algorithm applied to multilevel image thresholding," *The Scientific World Journal*, vol. 2014, pp. 1–16, 2014.
- [15] P. Szczypinski, A. Klepaczko, M. Pazurek, and P. Daniel, "Texture and color based image segmentation and pathology detection in capsule endoscopy videos," *Computer methods and programs in biomedicine*, vol. 113, no. 1, pp. 396–411, 2014.
- [16] Y. Fu, W. Zhang, M. Mandal, and M. Q.-H. Meng, "Computer-aided bleeding detection in WCE video," *IEEE journal of biomedical and health informatics*, vol. 18, no. 2, pp. 636–642, 2014.
- [17] S. Sawant and M. Deshpande, "Tumor recognition in wireless capsule endoscopy images," *International Journal of Computer Science and Network Security (IJCSNS)*, vol. 15, no. 4, pp. 85–89, 2015.

- [18] B. Li, G. Xu, R. Zhou, and T. Wang, "Computer aided wireless capsule endoscopy video segmentation," *Medical physics*, vol. 42, no. 2, pp. 645–652, 2015.
- [19] Y. Jia, "Polyps auto-detection in wireless capsule endoscopy images using improved method based on image segmentation," in *IEEE International Conference on Robotics and Biomimetics (ROBIO)*. IEEE, 2015, pp. 1631–1636.
- [20] J. Silva, A. Histace, O. Romain, X. Dray, and B. Granado, "Toward embedded detection of polyps in WCE images for early diagnosis of colorectal cancer," *International Journal of Computer Assisted Radiology and Surgery*, vol. 9, no. 2, pp. 283–293, 2014.
- [21] G. Liu, G. Yan, S. Kuang, and Y. Wang, "Detection of small bowel tumor based on multi-scale curvelet analysis and fractal technology in capsule endoscopy," *Computers in biology and medicine*, vol. 70, pp. 131–138, 2016.
- [22] F. Deeba, F. M. Bui, and K. A. Wahid, "Automated growcut for segmentation of endoscopic images," in *2016 International Joint Conference on Neural Networks (IJCNN)*. IEEE, 2016, pp. 4650–4657.
- [23] S. Hwang and M. E. Celebi, "Polyp detection in wireless capsule endoscopy videos based on image segmentation and geometric feature," in *2010 IEEE International Conference on Acoustics, Speech and Signal Processing*, March 2010, pp. 678–681.
- [24] A. Karargyris and N. Bourbakis, "Detection of small bowel polyps and ulcers in wireless capsule endoscopy videos," *IEEE Transactions on Biomedical Engineering*, vol. 58, no. 10, pp. 2777–2786, Oct 2011.
- [25] L. Yu, P. C. Yuen, and J. Lai, "Ulcer detection in wireless capsule endoscopy images," in *21st International Conference on Pattern Recognition (ICPR)*, Nov 2012, pp. 45–48.
- [26] V. S. Charisis, L. J. Hadjileontiadis, C. N. Liatsos, C. C. Mavrogiannis, and G. D. Sergiadis, "Capsule endoscopy image analysis using texture information from various colour models," *Computer methods and programs in biomedicine*, vol. 107, no. 1, pp. 61–74, 2012.
- [27] R. Kumar, Q. Zhao, S. Seshamani, G. Mullin, G. Hager, and T. Dasopoulos, "Assessment of Crohn's disease lesions in wireless capsule endoscopy images," *IEEE Transactions on Biomedical Engineering*, vol. 59, no. 2, pp. 355–362, Feb 2012.
- [28] B. Li and M. Q. H. Meng, "Tumor recognition in wireless capsule endoscopy images using textural features and SVM-based feature selection," *IEEE Transactions on Information Technology in Biomedicine*, vol. 16, no. 3, pp. 323–329, May 2012.
- [29] H. Chen, J. Chen, Q. Peng, G. Sun, and T. Gan, "Automatic hookworm image detection for wireless capsule endoscopy using hybrid color gradient and contourlet transform," in *2013 6th International Conference on Biomedical Engineering and Informatics*. IEEE, 2013, pp. 116–120.
- [30] L. Cui, C. Hu, Y. Zou, and M. Q. H. Meng, "Bleeding detection in wireless capsule endoscopy images by support vector classifier," in *IEEE International Conference on Information and Automation (ICIA)*, June 2010, pp. 1746–1751.
- [31] S. Sainju, F. M. Bui, and K. Wahid, "Bleeding detection in wireless capsule endoscopy based on color features from histogram probability," in *26th Annual IEEE Canadian Conference on Electrical and Computer Engineering (CCECE)*, May 2013, pp. 1–4.
- [32] G. Lv, G. Yan, and Z. Wang, "Bleeding detection in wireless capsule endoscopy images based on color invariants and spatial pyramids using support vector machines," in *Annual International Conference of the IEEE Engineering in Medicine and Biology Society*, Aug 2011, pp. 6643–6646.
- [33] A. K. Kundu, M. N. Rizve, T. Ghosh, S. A. Fattah, and C. Shahnaz, "A histogram based scheme in YIQ domain for automatic bleeding image detection from wireless capsule endoscopy," in *2015 IEEE International WIE Conference on Electrical and Computer Engineering (WIECON-ECE)*, Dec 2015, pp. 455–458.
- [34] C.-C. Chang and C.-J. Lin, "LIBSVM: A library for support vector machines," *ACM Transactions on Intelligent Systems and Technology*, vol. 2, no. 3, pp. 27:1–27:27, May 2011.
- [35] C.-W. Hsu, C.-C. Chang, and C.-J. Lin, "A practical guide to support vector classification," National Taiwan University, Tech. Rep., 2010.
- [36] F. Deeba, "Bleeding images and corresponding ground truth of CE images," 2016. [Online]. Available: <https://sites.google.com/site/farahdeeba073/Research/resources>
- [37] L. R. Dice, "Measures of the amount of ecologic association between species," *Ecology*, vol. 26, no. 3, pp. 297–302, 1945.
- [38] H. Zhou, G. Schaefer, A. H. Sadka, and M. E. Celebi, "Anisotropic mean shift based fuzzy c-means segmentation of dermoscopy images," *IEEE Journal of Selected Topics in Signal Processing*, vol. 3, no. 1, pp. 26–34, 2009.